

# Wormlike Micelles Formed by Synergistic Self-Assembly in Mixtures of Anionic and Cationic Surfactants

Srinivasa R. Raghavan,\* Gerhard Fritz, and Eric W. Kaler

Center for Molecular and Engineering Thermodynamics, Department of Chemical Engineering, University of Delaware, Newark, Delaware 19716

Received October 15, 2001. In Final Form: January 28, 2002

Self-assembly in mixtures of cationic and anionic surfactants occurs synergistically because of attractive interactions between the oppositely charged headgroups. Here, such effects are exploited to obtain highly viscoelastic fluids at low total surfactant concentration. The systems considered are mixtures of the  $C_{18}$ -tailed anionic surfactant, sodium oleate (NaOA), and cationic surfactants from the trimethylammonium bromide family ( $C_n$ TAB). In particular, mixtures of NaOA and  $C_8$ TAB show remarkably high viscosities: for 3% surfactant, the zero-shear viscosity  $\eta_0$  peaks at ca. 1800 Pa·s for a weight ratio of 70/30 NaOA/ $C_8$ TAB. The high viscosities reflect the growth of giant, entangled wormlike micelles in the solutions. Mixtures of NaOA with a shorter-chain analogue ( $C_6$ TAB) have much lower viscosities, indicating a weak micellar growth and hence a weak attraction between the surfactants. On the other hand, increasing the  $C_n$ TAB tail length to  $n = 10$  or  $12$  leads to much stronger interactions between these surfactants and NaOA. Consequently, both micellar and bilayer structures are formed in these mixtures, and the samples separate into two or more phases over a wide composition range. Thus, the synergistic growth of wormlike micelles in cationic/anionic mixtures is maximized when there is an optimal asymmetry in the surfactant tail lengths.

## Introduction

Over the past 15 years, the self-assembly of ionic surfactants into wormlike micelles has been widely investigated.<sup>1–3</sup> Wormlike micelles are typically formed by adding salt to solutions of a cationic surfactant such as cetyltrimethylammonium bromide ( $C_{16}$ TAB). The salt facilitates micellar growth by screening the electrostatic repulsions between the charged surfactant headgroups. Much like polymers, wormlike micelles tend to be long and flexible chains (contour lengths of ca. 1  $\mu$ m) that become entangled into a transient network, thereby imparting viscoelasticity to the solution. The micelles can thus be exploited for thickening and rheology-control applications in aqueous systems.

Mixtures of surfactants can exhibit synergistic gains compared to the parent surfactants in both surface and bulk properties.<sup>4–10</sup> This is particularly true when there are attractive interactions between the surfactants, as is the case in mixtures of anionic and cationic surfactants. For example, adding small amounts of the anionic surfactant sodium dodecyl benzenesulfonate (SDBS) to

solutions of the cationic surfactant cetyltrimethylammonium tosylate ( $C_{16}$ TAT) causes a synergistic enhancement of the rheological properties.<sup>8</sup> Note that  $C_{16}$ TAT has a hydrophobic counterion that binds strongly to the micelle, thereby promoting micellar growth. Thus,  $C_{16}$ TAT by itself forms wormlike micelles, and the resulting solutions are viscous.<sup>11</sup> Adding SDBS to  $C_{16}$ TAT increases the zero-shear viscosity  $\eta_0$  10-fold, with the peak occurring at a weight ratio of 4/96 SDBS/ $C_{16}$ TAT.<sup>8</sup> Further addition of SDBS lowers  $\eta_0$ , and for SDBS/ $C_{16}$ TAT ratios exceeding 9/91, the samples separate into two phases.<sup>8</sup> At even higher SDBS fractions, bilayer phases (vesicles or lamellae) coexist with micellar solutions, and a crystalline precipitate forms at the equimolar composition.<sup>4</sup>

The above studies illustrate how strong interactions between headgroups in cationic/anionic mixtures can facilitate micellar growth as well as cause phase separation. The micelles grow at low SDBS content because SDBS reduces the surface potential of the mixed micelles via charge neutralization, while the released counterions increase the ionic strength.<sup>8</sup> At higher SDBS content, however, the strongly bound cationic–anionic pair acts like a double-chained zwitterion and packs preferentially into bilayer geometries.<sup>4</sup> At the equimolar ratio, the catanionic surfactant  $C_{16}TA^+DBS^-$  (i.e., the compound formed by eliminating the counterions from the two surfactants) precipitates out of the solution.<sup>4</sup>

Previous studies of cationic/anionic mixtures<sup>12–18</sup> suggest that phase separation and precipitation can be avoided if the surfactants contain one long and one short alkyl tail. For example, dodecyltrimethylammonium

\* To whom correspondence should be addressed: e-mail sraghava@eng.umd.edu; Tel (301) 405-8164; FAX (301) 405-0523.

(1) Cates, M. E.; Candau, S. J. *J. Phys.: Condens. Matter* **1990**, *2*, 6869.

(2) Rehage, H.; Hoffmann, H. *Mol. Phys.* **1991**, *74*, 933.

(3) Candau, S. J.; Oda, R. *Colloids Surf.* **2001**, *183*, 5.

(4) Kaler, E. W.; Herrington, K. L.; Murthy, A. K.; Zasadzinski, J. A. N. *J. Phys. Chem.* **1992**, *96*, 6698.

(5) Herrington, K. L.; Kaler, E. W.; Miller, D. D.; Zasadzinski, J. A.; Chiruvolu, S. *J. Phys. Chem.* **1993**, *97*, 13792.

(6) Brasher, L. L.; Herrington, K. L.; Kaler, E. W. *Langmuir* **1995**, *11*, 4267.

(7) Yatecilla, M. T.; Herrington, K. L.; Brasher, L. L.; Kaler, E. W.; Zasadzinski, J. A. *J. Phys. Chem.* **1996**, *100*, 5874.

(8) Koehler, R. D.; Raghavan, S. R.; Kaler, E. W. *J. Phys. Chem.* **2000**, *104*, 11035.

(9) Holland, P. M., Rubingh, D. N., Eds.; *Mixed Surfactant Systems*; ACS Symposium Series 501; American Chemical Society: Washington, DC, 1992; Chapters 1 and 2.

(10) Rosen, M. J. In *Mixed Surfactant Systems*; ACS Symposium Series 501; Holland, P. M., Rubingh, D. N., Eds.; American Chemical Society: Washington, DC, 1992; pp 316–326.

(11) Soltero, J. F. A.; Puig, J. E. *Langmuir* **1996**, *12*, 2654.

(12) Regev, O.; Khan, A. *J. Colloid Interface Sci.* **1996**, *182*, 95.

(13) Edlund, H.; Sadaghiani, A.; Khan, A. *Langmuir* **1997**, *13*, 4953.

(14) Barker, C. A.; Saul, D.; Tiddy, G. J. T.; Wheeler, B. A.; Willis, E. *J. Chem. Soc., Faraday Trans. 1* **1974**, *70*, 154.

(15) Kato, T.; Iwai, M.; Seimiya, T. *J. Colloid Interface Sci.* **1989**, *130*, 439.

(16) Huang, J. B.; Zhao, G. X. *Colloid Polym. Sci.* **1995**, *273*, 156.

(17) Zhao, G. X.; Xiao, J. X. *Colloid Polym. Sci.* **1995**, *273*, 1088.

(18) Talhout, R.; Engberts, J. B. F. N. *Langmuir* **1997**, *13*, 5001.

chloride (C<sub>12</sub>TAC) and sodium nonanoate (SN) form isotropic micellar solutions at all compositions up to 40 wt % surfactant.<sup>12</sup> Tail length asymmetry does not necessarily preclude phase separation, though, for example, mixtures of sodium dodecyl sulfate (SDS) and octyltrimethylammonium bromide (C<sub>8</sub>TAB) form two phases over a range of compositions,<sup>14,15</sup> as do mixtures of C<sub>12</sub>TAC and sodium perfluorononanoate<sup>12</sup> (the fluorocarbon counterpart of SN). Significantly, many of the above mixtures do show a higher viscosity relative to the pure component solutions.<sup>12,14</sup> For instance, in the C<sub>12</sub>TAC/SN system, adding SN to C<sub>12</sub>TAC at 10% total surfactant increased the viscosity 50-fold to a peak at the equimolar ratio.<sup>12</sup> The viscosity rise correlated with the growth of micelles from spheres to rods of axial ratio about 10.

Here, we report cationic/anionic mixtures that exhibit a *million-fold increase* in viscosity relative to the single-component solutions. The anionic surfactant in this case is sodium oleate (NaOA), which has a C<sub>18</sub> alkyl tail containing a cis unsaturation. The cationic surfactants are from the alkyl trimethylammonium bromide (C<sub>*n*</sub>TAB) family having linear alkyl tails ranging from 6 to 12 carbons. We show that the phase behavior and rheology of NaOA/C<sub>*n*</sub>TAB mixtures can be tuned by a judicious combination of surfactant tail lengths.

### Experimental Section

Alkyltrimethylammonium bromide surfactants (C<sub>*n*</sub>H<sub>2*n*+1</sub>N-(CH<sub>3</sub>)<sub>3</sub>Br) with *n*-hexyl, *n*-octyl, *n*-decyl, and *n*-dodecyl tails were obtained from TCI America (all were of 99+% purity). Sodium oleate (*cis*-9-octadecanoate, C<sub>9</sub>H<sub>18</sub>=C<sub>8</sub>H<sub>15</sub>COONa), also from TCI America, was of 97+% purity. All surfactants were used as received. Distilled–deionized water was used in preparing the mixed surfactant solutions. Samples were equilibrated at 25 °C for phase behavior observations, and phase boundaries were identified visually.

Rheological experiments (steady and dynamic) were conducted at 25 °C on the single-phase samples. The experiments were performed on a Bohlin rheometer using a couette cell (cup of 27.5 mm o.d., bob of 25 mm i.d., and 37.5 mm length) or a cone-and-plate apparatus (40 mm diameter, 4° cone angle). For mildly viscous samples, the viscosity was measured using a Cannon-Ubbelohde capillary viscometer immersed in a constant temperature water bath at 25 °C. Flow times were sufficiently high in all cases so that kinetic energy corrections were not necessary.

Small-angle neutron scattering (SANS) experiments were performed at the National Institute of Standards and Technology (NIST) in Gaithersburg, MD, on the NG-3 beamline. The incident neutron wavelength was 6 Å with a 15% spread. Quartz cells with 2 mm path lengths were used, and the samples were placed in a temperature-controlled chamber maintained at 25 °C. Three different sample-to-detector distances were used to span a range of 0.004–0.4 Å<sup>-1</sup> in the scattering vector *q*. The scattering spectra were corrected for background radiation, detector efficiency, empty cell scattering, and sample transmission. The spectra were radially averaged and placed on an absolute scale using calibration standards provided by NIST. The data are shown in terms of the absolute scattered intensity *I* as a function of the scattering vector *q* = (4π/λ) sin(θ/2), where λ is the wavelength of incident neutrons and θ the scattering angle.

### Results

**Phase Behavior and Rheology.** Consider mixtures of NaOA and octyltrimethylammonium bromide (C<sub>8</sub>TAB) at a total surfactant concentration of 3 wt %. Because of its long (C<sub>18</sub>) alkyl tail, NaOA self-assembles readily in aqueous solution, and its critical micelle concentration (cmc) is low (0.06 wt %).<sup>20</sup> On the other hand, the shorter

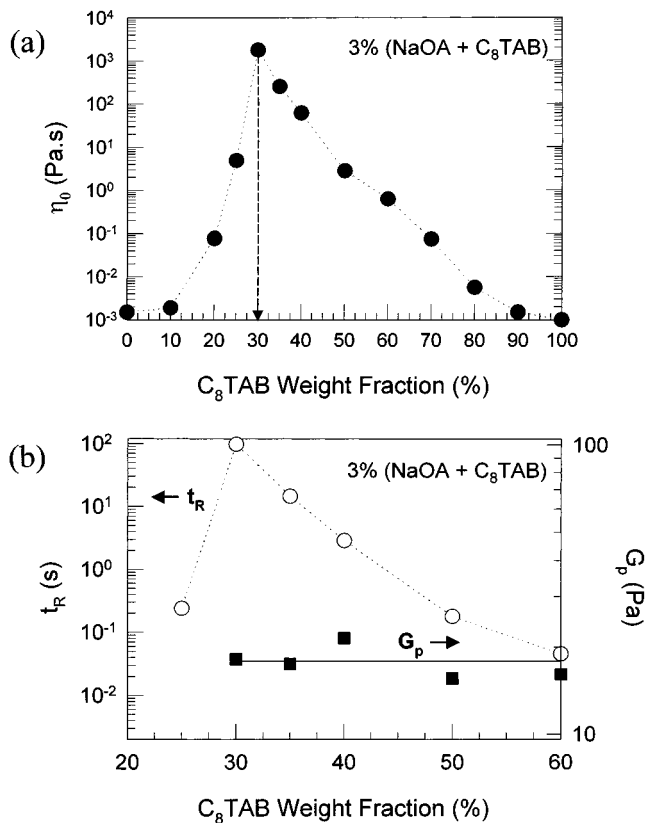


**Figure 1.** Rheology of NaOA/C<sub>8</sub>TAB mixtures as a function of composition for a total surfactant content of 3 wt %: (a) zero-shear viscosity  $\eta_0$ ; (b) relaxation time  $t_R$  and plateau modulus  $G_p$ .

tail in C<sub>8</sub>TAB leads to a much higher cmc (3.5 wt %).<sup>20</sup> Thus, at a concentration of 3 wt %, C<sub>8</sub>TAB does not micellize in solution whereas NaOA tends to form small micelles. Globular or short, rodlike micelles have a weak effect on the rheology—the solutions are Newtonian, and the viscosity rises linearly with the volume fraction of the micelles ( $\phi$ ) according to<sup>21</sup>

$$\eta = \eta_m(1 + [\eta]\phi) \quad (1)$$

where  $\eta_m$  is the viscosity of the solvent medium (for water at 25 °C,  $\eta_m$  is 1 mPa·s). The intrinsic viscosity  $[\eta]$  is 2.5 for a dispersion of hard spheres, while for short rods below the overlap concentration  $c^*$ ,  $[\eta]$  is a function of the micelle length  $\bar{L}$ .<sup>21</sup> The viscosity of the 3% NaOA solution is 1.5 mPa·s, indicating the presence of short rodlike micelles.

Adding a small amount of C<sub>8</sub>TAB to an NaOA solution increases the viscosity dramatically (Figure 1a). The zero-shear viscosity  $\eta_0$  of 3% surfactant solutions rises exponentially with increasing C<sub>8</sub>TAB fraction and peaks at a value of 1800 Pa·s for a composition of 70/30 NaOA/C<sub>8</sub>TAB. This is more than 6 orders of magnitude higher than the viscosities of the pure component solutions. The increase in viscosity reflects the growth of micelles from short, nonoverlapping rods (dilute regime, below  $c^*$ ) to long, flexible worms (semidilute regime, above  $c^*$ ).<sup>2</sup> These worms are expected to have average contour lengths  $\bar{L}$  of 1  $\mu$ m or higher. It is the entanglement of these worms into

(20) Mukerjee, P.; Mysels, K. J. *Critical Micelle Concentrations of Aqueous Surfactant Systems*; NSRDS-NBS-36; U.S. Government Printing Office: Washington, DC, 1971.

(21) Larson, R. G. *The Structure and Rheology of Complex Fluids*; Oxford University Press: Oxford, 1999.

(19) Jonsson, B.; Lindman, B.; Holmberg, K.; Kronberg, B. *Surfactants and Polymers in Aqueous Solution*; John Wiley & Sons: New York, 1998.

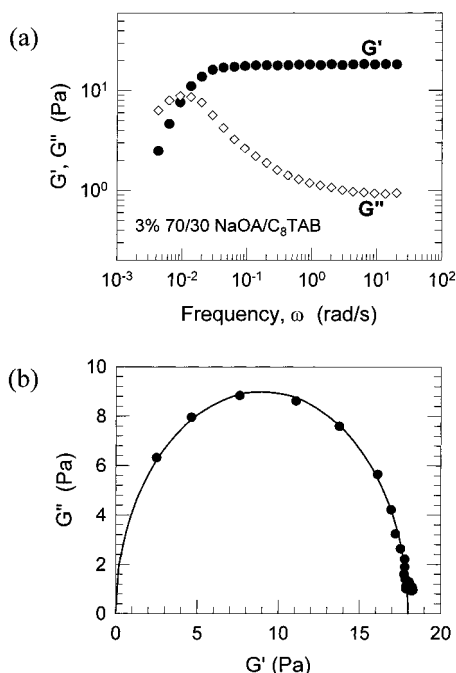


**Figure 2.** Dynamic rheology of a 3 wt % surfactant solution with the composition 70/30 NaOA/C<sub>8</sub>TAB: (a) dynamic frequency spectrum; (b) Cole–Cole plot.

a transient network that imparts viscoelasticity to the solutions.<sup>1,2</sup>

The synergistic formation of elongated micelles in 3% NaOA/C<sub>8</sub>TAB mixtures is apparent even when the mixture contains mostly C<sub>8</sub>TAB. For example, the viscosity of a 20/80 NaOA/C<sub>8</sub>TAB solution is 5 mPa·s (i.e., 5 times that of C<sub>8</sub>TAB alone), which suggests that rodlike micelles of moderate length ( $\bar{L} < 1/c^*$ ) are present. In turn, this confirms that the cmc of the 20/80 mixture is significantly lower than the cmc of C<sub>8</sub>TAB alone; i.e., a small amount of NaOA induces the C<sub>8</sub>TAB to comicellize.

The 3% NaOA/C<sub>8</sub>TAB mixtures also show viscoelastic behavior in dynamic shear. Dynamic rheological measurements of the elastic ( $G'$ ) and viscous ( $G''$ ) moduli as functions of frequency yield values of the plateau modulus  $G_p$  and the relaxation time  $t_R$  ( $t_R = 1/\omega_c$ , where  $\omega_c$  is the intersection point of  $G'$  and  $G''$ ). Figure 1b shows that the plateau modulus  $G_p$  is independent of composition, while  $t_R$  peaks at the composition of 70/30 NaOA/C<sub>8</sub>TAB, at which the zero-shear viscosity  $\eta_0$  also showed a peak.

Dynamic rheology also reveals that samples near the  $t_R$  maximum are Maxwell fluids, i.e., fluids with a single relaxation time. Figure 2a shows the frequency spectrum for the 70/30 NaOA/C<sub>8</sub>TAB sample, and a Cole–Cole plot of these data (Figure 2b) reveals the semicircle expected of a Maxwell fluid.<sup>1</sup> Steady-shear rheological data for the same sample (Figure 3) shows a Newtonian plateau for the viscosity at low shear rates, followed by shear thinning at higher shear rates. The zero-shear viscosity  $\eta_0$  is 1800 Pa·s, which correlates well with the product of  $t_R$  (100 s) and  $G_p$  (18 Pa; Figure 3a), as expected<sup>1</sup> for a Maxwell fluid. In the shear-thinning regime, the shear stress  $\sigma$  approaches a plateau.

The effect of total surfactant concentration on the rheology is studied next for a fixed composition of 70/30 NaOA/C<sub>8</sub>TAB (Figure 4). The zero-shear viscosity  $\eta_0$  shows a nonmonotonic behavior as a function of surfactant concentration, peaking at a concentration of about 4 wt %. For concentrations of 10% and higher,  $\eta_0$  drops to a low and nearly constant value (the dynamic response is weak

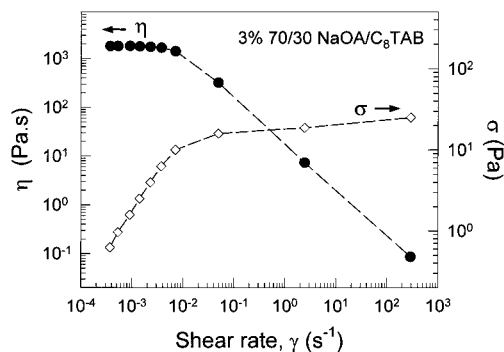


**Figure 3.** Steady-shear rheology of a 3 wt % surfactant solution with the composition 70/30 NaOA/C<sub>8</sub>TAB. The viscosity  $\eta$  and the shear stress  $\sigma$  are plotted as a function of the shear rate.

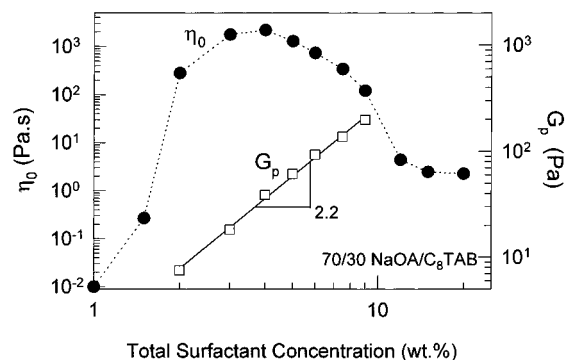


**Figure 4.** Rheology of NaOA/C<sub>8</sub>TAB mixtures as a function of total surfactant concentration. The ratio of NaOA/C<sub>8</sub>TAB is held constant at 70/30. Data for the zero-shear viscosity  $\eta_0$  and the plateau modulus  $G_p$  are shown.

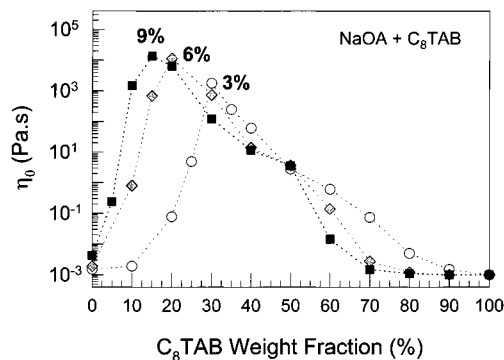


**Figure 5.** Zero-shear viscosity  $\eta_0$  of NaOA/C<sub>8</sub>TAB mixtures as a function of composition for three different surfactant concentrations (3, 6, and 9 wt %).

in these cases.) The plateau modulus  $G_p$ , on the other hand, monotonically increases with concentration. The power-law exponent for  $G_p$  is 2.2, which is exactly the value expected for entangled wormlike micelles.<sup>1</sup>

Concentration effects can alternately be probed by varying the mixture composition at different values of the total surfactant content. Plots of  $\eta_0$  vs the C<sub>8</sub>TAB fraction in the mixture at 3%, 6%, and 9% surfactant are shown in Figure 5. In each case there is a peak in  $\eta_0$ , and the peak position shifts to compositions richer in NaOA with increasing concentration. For a 50/50 NaOA/C<sub>8</sub>TAB sample ( $\approx$  equimolar ratio),  $\eta_0$  is practically unaltered over the concentration range. A small excess of either one of the surfactants causes  $\eta_0$  to drop with increasing concentration. Only at low C<sub>8</sub>TAB content does the viscosity increase with concentration.

The effect of added salt on the rheology is examined in Figure 6, where the viscosities of 3% surfactant solutions

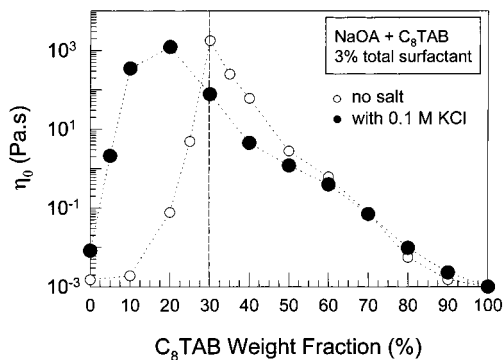


**Figure 6.** Rheology of NaOA/C<sub>8</sub>TAB mixtures in the presence of salt. The zero-shear viscosity  $\eta_0$  is plotted as a function of composition for mixtures containing 0.1 M KCl (filled circles). The data in the absence of salt are also shown for comparison (open circles). The total surfactant content is 3 wt % in all cases.

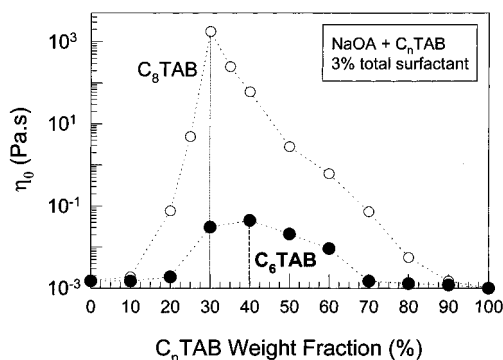


**Figure 7.** Zero-shear viscosity  $\eta_0$  of NaOA/C<sub>6</sub>TAB mixtures as a function of composition. For comparison, data for NaOA/C<sub>8</sub>TAB mixtures are also shown. The total surfactant content is 3 wt % in all cases.

in the presence of 0.1 M KCl are compared with those shown previously for solutions with no added salt. The presence of KCl increases the viscosity at low C<sub>8</sub>TAB content, while depressing it at or beyond the original viscosity peak (i.e., 70/30 NaOA/C<sub>8</sub>TAB). Beyond the equimolar ratio, the  $\eta_0$  in the presence of KCl approaches the earlier value. Thus, the viscosity peak apparently corresponds to an optimal extent of electrostatic screening, as discussed presently.

Finally, cationic surfactants (C<sub>*n*</sub>TAB) of varying alkyl tail lengths are examined in mixtures with the C<sub>18</sub>-tailed NaOA. First, the viscosities of 3% NaOA/C<sub>6</sub>TAB mixtures are compared with those for 3% NaOA/C<sub>8</sub>TAB (Figure 7). The NaOA/C<sub>6</sub>TAB system also describes a viscosity maximum; however, the  $\eta_0$  values are far lower than those of the NaOA/C<sub>8</sub>TAB system. The peak viscosity for 3% NaOA/C<sub>6</sub>TAB mixtures is only about 50 mPa·s, i.e., 50 times the viscosity of water. Thus, decreasing the alkyl tail length from eight to six units greatly reduces the synergism in self-assembly. Also, the peak in  $\eta_0$  is shifted to a composition of 60/40 NaOA/C<sub>6</sub>TAB, which is close to the equimolar ratio for this mixture.

In the case of 3% NaOA/C<sub>10</sub>TAB and 3% NaOA/C<sub>12</sub>TAB mixtures, samples at intermediate compositions separate into two or more phases (Figure 8). The nature of these phases has not been determined systematically; however, in most samples, one of the phases likely involves a lamellar morphology. Upon dilution, many samples turn into nonviscous, isotropic, one-phase solutions with a blue color—these are likely to contain unilamellar vesicles (~100 nm in diameter), and the blue color is due to the

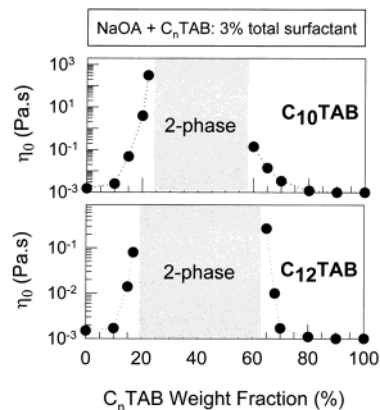


**Figure 8.** Zero-shear viscosity  $\eta_0$  as a function of composition for mixtures of NaOA/C<sub>10</sub>TAB and NaOA/C<sub>12</sub>TAB. The total surfactant content is 3 wt % in all cases. For intermediate compositions in both systems, the samples separate into two (or more) phases.

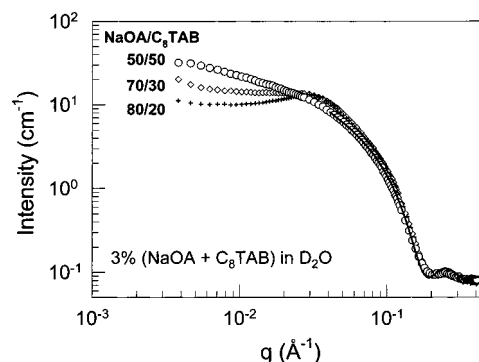


**Figure 9.** SANS spectra for 3 wt % NaOA/C<sub>8</sub>TAB solutions in D<sub>2</sub>O. The solid line is a fit to the 50/50 sample for  $q > 0.04 \text{ \AA}^{-1}$  using a model for monodisperse cylinders. From the fit, a micelle radius of 20 Å is obtained.

scattering of light by these entities.<sup>4</sup> Note also that the multiphase region spans a slightly larger composition range for the NaOA/C<sub>12</sub>TAB system than for the NaOA/C<sub>10</sub>TAB system. As regards the solution viscosity,  $\eta_0$  diverges as the phase boundary is approached from either side, with higher values of  $\eta_0$  being observed in the NaOA/C<sub>10</sub>TAB system than in the NaOA/C<sub>12</sub>TAB system.

**Small-Angle Neutron Scattering.** To further probe the microstructure, SANS measurements were performed on selected NaOA/C<sub>8</sub>TAB samples in D<sub>2</sub>O. SANS spectra ( $I$  vs  $q$ ) for three NaOA/C<sub>8</sub>TAB samples at 3 wt % total surfactant are shown in Figure 9. The compositions were chosen to mirror the nonmonotonic rheology—the 70/30 sample corresponds to a viscosity peak while the others fall on either side of this peak (the rheology in D<sub>2</sub>O is similar to that in H<sub>2</sub>O). The SANS data, however, show only a monotonic trend. The 80/20 and 70/30 samples show a peak at intermediate  $q$  and depressed scattering at low  $q$ , reflecting the electrostatic repulsions between the charged aggregates in solution (note that there is no salt added to screen the repulsions).<sup>8,22</sup> As the proportion of cationic surfactant increases, the peak becomes less pronounced, and for the 50/50 sample (close to equimolar ratio), the peak is absent. The 70/30 sample also shows a slight upturn in intensity at low  $q$ . The scattering at high  $q$  is approximately identical for the three samples.

SANS data for three different surfactant concentrations at a composition of 70/30 NaOA/C<sub>8</sub>TAB are shown in

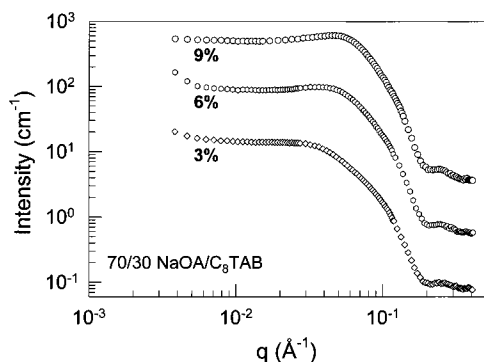


**Figure 10.** SANS spectra for 70/30 NaOA/C<sub>8</sub>TAB solutions in D<sub>2</sub>O at different surfactant concentrations. The data for the 3% sample are absolute values while the remaining curves are offset by factors of 5 for clarity.

Figure 10. A peak appears at intermediate  $q$  in all cases, and the peak position  $q_{\max}$  dictates the correlation length  $\xi = 2\pi/q_{\max}$  which represents the mean distance between the charged cylindrical micelles.<sup>22</sup> The shift in  $q_{\max}$  to higher  $q$  with increasing concentration means that  $\xi$  correspondingly decreases, as expected.<sup>8,22</sup> The other notable aspect is the upturn at low  $q$ , observed in both the 3% and 6% samples, but not in the 9% case. Such an upturn usually signifies the onset of attractive interactions or critical fluctuations.

### Discussion

**Analysis of SANS Data.** To obtain structural information, the SANS data have to be fitted to a model. The scattered intensity, in general, will have contributions from both the structure factor  $S(q)$  and the form factor  $P(q)$  of the elongated micelles.<sup>22</sup> Structure factor effects cannot be neglected here because the micellar charge is not screened completely and the micellar concentration is semidilute.<sup>23,24</sup> Analysis using the indirect Fourier transform (IFT) method<sup>25</sup> shows that  $S(q)$  effects are present even for the 50/50 sample, for which there is no interaction peak. This is also why the slope of  $I$  vs  $q$  at low  $q$  for this sample is not equal to  $-1$  as would be expected for rodlike micelles.

At high  $q$  where  $S(q)$  is approximately 1, the data admit to analysis based on the form factor  $P(q)$ . For the 50/50 sample, a fit of the high  $q$  data to the form factor for monodisperse cylinders (solid line, Figure 9) yields a micelle radius of ca. 20 Å. The micelle radius is found to vary negligibly with composition, and its value compares well with the length of an extended oleyl chain (~25 Å). More sophisticated analysis of the high  $q$  data using the cross-section IFT method confirms that the micelles are homogeneous with an average radius of  $19 \pm 1$  Å. However, the analysis also suggests a polydispersity of 9–15% in the micelle radius, which may actually imply slight deviations from a circular cross section, as reported for other cationic/anionic systems.<sup>23,24</sup> Taken together, the SANS analysis confirms the presence of micellar chains, whose cross section may be circular or slightly ellipsoidal. The length of these chains cannot be obtained unambiguously without accounting for  $S(q)$  effects.

### Wormlike Micelles in Mixed Surfactant Systems.

From the SANS measurements as well as from the rheology, it is evident that long wormlike micelles are

present in these mixed surfactant solutions. Signatures of wormlike micelles include the Maxwellian behavior in dynamic rheology (Figure 3), and the high viscosity and stress plateau in steady-shear rheology (Figure 4).<sup>1,2</sup> Visual observations (through cross-polars) also reveal that these isotropic solutions become birefringent under flow, which is another signature of elongated micelles.<sup>2</sup> The presence of wormlike micelles is further confirmed by cryo-TEM, as reported elsewhere.<sup>26</sup>

A noteworthy aspect of these viscous solutions is that the major component is an anionic surfactant (NaOA). Most reports of highly viscous wormlike micellar solutions have involved a long-tailed cationic surfactant.<sup>2,3</sup> Anionic surfactants have been shown to form elongated micelles previously,<sup>27,28</sup> but the zero-shear viscosities of those solutions were quite low ( $\eta_0 < 10$  Pa·s), and moreover, the micelles grew only when high concentrations of simple salts (e.g., KCl) were added. Here we have shown that it is sufficient to add a few mM of C<sub>8</sub>TAB to the anionic surfactant NaOA to produce high solution viscosities (comparable to adding a few mM of the hydrotrope sodium salicylate to a cationic surfactant such as C<sub>16</sub>TAB). Moreover, the zero-shear viscosity  $\eta_0$  is remarkably high ( $> 1000$  Pa·s) for many of the NaOA/C<sub>8</sub>TAB samples. These values are comparable to the highest viscosities obtained using cationic surfactants at equivalent surfactant concentrations.<sup>2</sup>

Why do long wormlike micelles form in cationic/anionic mixtures? The origin lies in the strong electrostatic interactions between the oppositely charged headgroups, as discussed above. To rationalize microstructures, it is useful to consider the surfactant packing parameter  $p = v/a_0l_c$ , where  $v$  is the tail volume,  $l_c$  the tail length, and  $a_0$  the area per headgroup.<sup>19,29</sup> The pairing of oppositely charged headgroups decreases the headgroup area  $a_0$  and thereby increases  $p$ . Thus, as the fraction of oppositely charged surfactant in the mixture increases,  $p$  varies from  $\sim 1/3$  for a single surfactant to  $\sim 1$  for the equimolar mixture. Correspondingly, the microstructure changes from spherical micelles to wormlike micelles to bilayer structures. This entire progression can be observed for NaOA/C<sub>10</sub>-TAB and NaOA/C<sub>12</sub>TAB mixtures.

The strong interaction between cationic and anionic headgroups also induces the catanionic salt to precipitate in mixtures close to the equimolar composition.<sup>9</sup> Particularly when the tail lengths of the cationic ( $n^+$ ) and anionic ( $n^-$ ) surfactants are nearly equal, the tails pack well in a crystalline lattice, and the precipitate is exceptionally stable.<sup>5</sup> Conversely, asymmetric tails do not pack efficiently, thereby inhibiting salt formation.<sup>12</sup> Here, the catanionic precipitate is formed at the equimolar composition for mixtures of NaOA ( $n^- = 18$ ) with C<sub>10</sub>TAB and C<sub>12</sub>TAB. However, for the NaOA/C<sub>6</sub>TAB and NaOA/C<sub>8</sub>-TAB systems, no precipitate is formed, and the samples are homogeneous micellar solutions over the composition range. Apparently, the asymmetry between the tails in the latter cases is sufficient to inhibit precipitation of the catanionic salt.

Similar trends in phase behavior have been reported previously for other cationic/anionic surfactant mixtures. For example, mixtures of C<sub>12</sub>TAB and sodium alkyl

(26) Edlund, H.; Norgren, M.; Raghavan, S. R.; Kaler, E. W. Manuscript in preparation.

(27) Gamboa, C.; Sepulveda, L. *J. Colloid Interface Sci.* **1986**, *113*, 566.

(28) Almgren, M.; Gimel, J. C.; Wang, K.; Karlsson, G.; Edwards, K.; Brown, W.; Mortensen, K. *J. Colloid Interface Sci.* **1998**, *202*, 222.

(29) Israelachvili, J. *Intermolecular and Surface Forces*; Academic Press: San Diego, 1991.

(23) Bergstrom, M.; Pedersen, J. S. *J. Phys. Chem. B* **1999**, *103*, 8502.

(24) Bergstrom, M.; Pedersen, J. S. *Phys. Chem. Chem. Phys.* **1999**, *1*, 4437.

(25) Supporting information for this paper.

carboxylates form a single micellar phase over the composition range for  $n^- = 8$  but separate into two coexisting liquid phases for  $n^- = 10$ .<sup>16</sup> Mixtures of C<sub>12</sub>-TAC and sodium nonanoate ( $n^- = 9$ ) form a single micellar phase at all compositions up to ~40 wt % surfactant.<sup>12</sup> Thus, asymmetry in the alkyl tail lengths promotes a stable micellar phase at the expense of bilayers and salt precipitates. For a constant ratio of tail lengths, increasing the total number of carbons in the tails (i.e.,  $n^{\text{tot}} = n^- + n^+$ ) enhances precipitation.<sup>9</sup> For example, bilayers and multiphase regions are predominant in the ternary phase diagram of C<sub>16</sub>TAB and sodium octyl sulfate ( $n^{\text{tot}} = 24$ ).<sup>6,7</sup> The comparative stability of the NaOA/C<sub>8</sub>TAB system ( $n^{\text{tot}} = 26$ ) is probably due to the cis double bond in the C<sub>18</sub> tail of NaOA, which hinders crystal packing.

**Mixed Surfactant Phase Behavior Based on the  $\beta$  Parameter.** From a macroscopic standpoint, interactions between surfactants can be quantified using the  $\beta$  parameter from regular solution theory.<sup>9,19</sup> For mixtures of two surfactants, 1 and 2,  $\beta$  is defined by<sup>9</sup>

$$\beta = \frac{W_{11} + W_{22} - 2W_{12}}{RT} \quad (2)$$

where  $W_{11}$ ,  $W_{22}$ , and  $W_{12}$  are the molar free energies of interaction for 1–1, 2–2, and 1–2 pairs, respectively. Ideal behavior implies no net interactions between the surfactants, i.e.,  $W_{11} = W_{22} = W_{12}$  and hence  $\beta = 0$ . On the other hand, attractive interactions between the surfactants implies that  $W_{12}$  will exceed  $W_{11}$  and  $W_{22}$  and  $\beta$  will hence be negative. In that case, the cmc's of the mixtures will be lower than those of the pure surfactants.<sup>9</sup>

The  $\beta$  parameter for a mixture of two surfactants can be estimated from cmc data as a function of mixture composition. As expected, cationic/anionic mixtures show negative values of  $\beta$ , and the more negative the  $\beta$ , the stronger the attractive interactions.<sup>9</sup> As the total number of alkyl carbons ( $n^{\text{tot}}$ ) increases,  $\beta$  becomes more negative.<sup>8</sup> For example, symmetric mixtures of C<sub>*n*</sub>SO<sub>4</sub>Na (alkyl sulfates, anionic) and C<sub>*n*</sub>TABs (cationic) exhibit  $\beta = -10.5$  for  $n = 8$ ,  $\beta = -18.5$  for  $n = 10$ , and  $\beta = -25.5$  for  $n = 12$ . In this series, precipitation of catanionic salt occurs at the equimolar composition for  $n = 10$  and 12, but not for  $n = 8$ . So moderately negative  $\beta$  leads to micellar growth, while highly negative  $\beta$  leads to bilayers and precipitation.

We can now classify the behavior of NaOA/C<sub>*n*</sub>TAB mixtures for different values of  $n$  in terms of expected values of  $\beta$ . First, consider the NaOA/C<sub>6</sub>TAB system where there is a large disparity between  $n^-$  and  $n^+$ . C<sub>6</sub>TAB, due to its weak amphiphilicity (it does not have a cmc), should be viewed as a hydrotropic salt rather than a surfactant. Consequently, NaOA and C<sub>6</sub>TAB will interact rather weakly ( $\beta$  expected to be ca.  $-5$ ). Adding C<sub>6</sub>TAB to NaOA will therefore have a weak effect on the surfactant packing parameter  $p$ , which may increase slightly from  $1/3$  to less than  $1/2$ . This correlates with weak micellar growth and hence a small rise in viscosity (Figure 9). Note that the peak in viscosity occurs near the equimolar ratio, where the micellar charge is screened the most. Similar results have been reported for C<sub>12</sub>TAC/sodium nonanoate mixtures,<sup>12</sup> where also the peak viscosity was low (30 mPa·s at 10 wt % surfactant), and the peak occurred at the equimolar composition.

Next, consider the NaOA/C<sub>10</sub>TAB and NaOA/C<sub>12</sub>TAB systems. Here,  $n^-$  and  $n^+$  are relatively close, and so the surfactant pairs should interact strongly ( $\beta$  expected to be around  $-20$ ). In turn, the packing parameter  $p$  will attain values close to 1 over a range of mixture compositions. This explains the existence of bilayer phases in these

mixtures (Figure 10). Note that bilayers occur over a wider composition range in the case of the longer-tailed C<sub>12</sub>-TAB. The catanionic salt also precipitates at the equimolar composition in each case. The viscosity increase on approaching the micelle–bilayer phase boundary reflects a change in  $p$  from  $1/3$  to  $1/2$  at those compositions.

Finally, consider the NaOA/C<sub>8</sub>TAB system. As in the NaOA/C<sub>6</sub>TAB case, the  $n^-$  and  $n^+$  are sufficiently different so that the mixtures are able to avoid phase separation or precipitation. However, C<sub>8</sub>TAB is far more amphiphilic than C<sub>6</sub>TAB and shows a cmc around 3.5 wt %. Therefore, relatively strong interactions should occur between NaOA and C<sub>8</sub>TAB (the  $\beta$  parameter is expected to be around  $-15$ ). Accordingly, the packing parameter  $p$  will assume values around  $1/2$  (but will not approach 1). This can explain the growth of giant wormlike micelles within the single-phase, homogeneous solutions. From a rheological perspective, such a mixture provides the optimal synergism.

**Interpretation of Viscosity Maxima.** We now address the viscosity maxima in NaOA/C<sub>8</sub>TAB mixtures as a function of composition (Figures 1, 5, and 6). Generally, these peaks appear at low C<sub>8</sub>TAB contents, well before the equimolar ratio (e.g., the peak at 3% surfactant occurs when there is roughly one C<sub>8</sub>TAB molecule for every two NaOA molecules in the micelle.) Thus, the peak does not reflect an optimal extent of charge neutralization. Why then does the viscosity go through a maximum? A plausible hypothesis is that there is a transition from linear to branched micelles at the peak.<sup>8,30</sup> According to this hypothesis, micelles grow linearly before the peak composition and are longest at the peak. Thereafter, the micelles tend to form branches rather than continue growing axially. As branching proceeds, the viscosity drops because the branch points are not fixed but are free to slide along the micelle (thereby providing an additional mode for stress relaxation).<sup>30</sup>

An attractive hypothesis is that the point of micellar branching represents a delicate balance in the electrostatic character of the system. For branching to occur, a 3-fold micellar junction must be energetically more favorable than a micellar end-cap.<sup>8</sup> This seems to be the case when the electrostatic interactions are sufficiently screened. Note that electrostatic screening can occur in two ways in these surfactant mixtures: (a) due to pairing of the oppositely charged headgroups within the micelle, which reduces the charge density at the micellar surface, and (b) due to the release of surfactant counterions into the solution, which serves to reduce the electrostatic double layer around each micelle. The former effect increases along a concentration path from pure surfactant to equimolar mixtures, while the latter effect increases with total surfactant concentration.

If indeed the viscosity peak corresponds to the onset of micellar branching, the shift in the peak position with surfactant concentration (Figure 6) and salt addition (Figure 7) can be rationalized. Adding salt (KCl) uniformly increases the ionic strength, so the extent of electrostatic screening is increased at all compositions. The onset of micellar branching hence occurs for a lower micellar surface charge, i.e., for a lower C<sub>8</sub>TAB content. Increasing the surfactant concentration increases the concentration of counterions released into the solution. The effect is thus similar to salt addition, and branching is initiated at a lower C<sub>8</sub>TAB content for a higher surfactant concentration.

(30) Lequeux, F. Reptation of connected worms. *Europhys. Lett.* **1992**, *19*, 675.

### Conclusions

Attractive interactions in mixtures of cationic and anionic surfactants are governed chiefly by the surfactant tail lengths. Generalizing the results from this study, three possible scenarios can be distinguished in terms of the tail lengths. First, if there is one long and one very short tail (e.g., NaOA + C<sub>6</sub>TAB), weak interactions ensue between the surfactants, leading to weak micellar growth (and a small rise in viscosity). Second, if both tails are long (e.g., NaOA + C<sub>12</sub>TAB), strong attractive interactions occur, leading to precipitation of the catanionic salt at the equimolar composition and the formation of bilayer structures over a significant window of compositions. Last, and most important, is the scenario where one tail is long and the other is of moderate length (e.g., NaOA + C<sub>8</sub>-TAB)—in this case, the attractive interactions are strong

enough to cause dramatic micellar growth, but not strong enough to induce bilayer structures or phase separation. The result is a dramatic enhancement of the rheological properties at intermediate compositions.

**Acknowledgment.** We acknowledge NIST for facilitating the SANS experiments performed as part of this work. Helpful discussions with Dr. Hakan Edlund (Mid-Sweden University, Sundsvall) are also acknowledged.

**Supporting Information Available:** Analysis of SANS data using the indirect Fourier transformation technique. This material is available free of charge via the Internet at <http://pubs.acs.org>.

LA0115583